STUDIA UBB PHYSICA, Vol. 61 (LXI), 2, 2016, pp. 83-90
(RECOMMENDED CITATION)

Dedicated to Professor Dr. Sorin Dan Anghel on His 65th Anniversary

STRUCTURAL AND MAGNETIC CHARACTERIZATION OF Fe_3O_4 NANOPARTICLES SYNTHESIZED AT ROOM TEMPERATURE

GABRIELA SOUCA[a], S. MICAN[a], A. STEFANCU[a,b], V. CHIȘ[a], R. TETEAN[a], N. LEOPOLD[a,b*]

ABSTRACT. Magnetite nanoparticles without surfactants were obtained by room temperature synthesis. X-ray diffraction data show that the nanoparticles crystallize in a cubic single phase structure. An average crystallite size of around 24 nm was calculated. The obtained Fe_3O_4 nanoparticles are ferrimagnetic at 4 K and at 300 K, too. It was shown that a ferrimagnetic to superparamagnetic transition is present, even if the superparamagnetic state is not pure. We assume that the true long-range ferromagnetic coupling is absent due to the small grain size of the sample.

Keywords: *magnetite nanoparticles, X-ray diffraction, magnetization*

INTRODUCTION

Among engineered nanomaterials, magnetic nanoparticles (MNPs) offer promising possibilities in biomedical field, due to their unique physico-chemical properties, including biocompatibility and magnetic properties that allow them to be manipulated by an external magnetic field gradient [1]. Particularly, nanoparticles made of a ferro- or ferrimagnetic material, i.e., iron oxide nanoparticles (ION), can exhibit a unique form of magnetism called superparamagnetism. This appears when the ION size is below a critical value – depending on the material, but typically around 10 – 20 nm - and the temperature is above a particular temperature which is called

[a] *Faculty of Physics, Babeş-Bolyai University, Kogălniceanu 1, 400084 Cluj-Napoca, Romania*
[b] *IMOGEN Research Institute, County Clinical Emergency Hospital, Pasteur f.n., 400006 Cluj-Napoca, Romania*
[*] *Corresponding author: nicolae.leopold@phys.ubbcluj.ro*

the blocking temperature (T_B) [1, 2]. In the superparamagnetic state, the magnetic moments of the nanoparticles fluctuate around the easy axes of magnetization. Thus, each of the MNPs will possess a large magnetic moment that continuously changes orientation. When a magnetic field is applied, MNPs in the superparamagnetic state display a fast response to the changes of the magnetic field without remnant (residual) magnetization. Therefore, in the superparamagnetic state, an MNP behaves as a paramagnetic atom with a giant spin [2]. This superparamagnetic behavior is highly useful in biomedicine for several applications such as contrast agents for magnetic resonance imaging (MRI), sensitizers in hyperthermal methods for cancer treatment, magnetic drug delivery or magnetic biosensors [1, 2].

EXPERIMENTAL

Synthesis of Fe_3O_4 magnetic nanoparticles

A previously reported method was used for synthesis of Fe_3O_4 MNPs without surfactants, at room temperature [3]. Briefly, deionized water (200 ml) was deoxygenated by bubbling nitrogen gas for 1 h in the solution. Afterwards, 25 ml of NH_4OH (1 M) was added and the mixture was stirred with mechanical agitation at 1000 rpm. Then, 1.352 g of $FeCl_3 \cdot 6H_2O$ and 0.695 g $FeSO_4 \cdot 7H_2O$ were separately dissolved in 20 ml and 10 ml deionized and deoxygenated water, respectively. Subsequently, amounts of 10 ml ferrous sulfate and 20 ml ferric chloride solutions were added to the ammonium hydroxide solution and the reaction mixture was stirred for 2.5 min at 1000 rpm. A black precipitate formed (Fig. 1) which was washed four times with deionized water. Finally, the prepared Fe_3O_4 MNPs were separated from the solution with a magnet [4]. Powder samples were obtained by drying on a glass slide, at room temperature.

Fig. 1. Photography of the Fe_3O_4 nanoparticles after synthesis.

X-ray diffraction measurements

The X-ray diffraction (XRD) measurements were performed on powder samples, at room temperature using a Bruker D8 Advance diffractometer with Bragg-Brentano focusing geometry and Cu K_α radiation. The average crystallite size was determined from the full width at half-maximum (FWHM) values of the XRD peaks using the Williamson-Hall method [5]. This method separates size and strain broadening and gives a more accurate value of the average crystallite size [5]. The FWHM values were obtained by fitting each XRD peak using a normalized pseudo-Voigt function. The instrumental broadening, measured from the XRD pattern of a LaB_6 reference sample, was subtracted from the obtained FWHM values. The lattice parameters were determined using Powdercell software version 2.3 made by the Federal Institute for Materials Research and Testing (BAM), Berlin.

Magnetic measurements

The magnetic measurements between 4 and 300 K were performed using a vibrating sample magnetometer (VSM) made by Cryogenic Limited in applied fields up to 2 T. Both zero-field-cooled (ZFC) and field-cooled (FC) measurements were performed [6]. The saturation magnetization values, M_S, were determined from magnetization curves using the approach to saturation law:

$$M = M_S\left(1-\frac{b}{H}\right)+\chi_0 H \tag{1}$$

where by b we denoted the coefficient of magnetic hardness and by χ_0 a Pauli-type contribution.

RESULTS AND DISCUSSION

Conventionally, magnetite is prepared by adding a base to an aqueous mixture of Fe^{2+} and Fe^{3+} salt at a 1:2 molar ratio [7]. The overall reaction of Fe_3O_4 precipitation may be written as follows:

$$Fe^{2+} + 2Fe^{3+} + 8OH^- \rightarrow Fe_3O_4 + H_2O \tag{2}$$

The maintaining of a non-oxidizing, oxygen-free environment is critical, otherwise, Fe_3O_4 might also be oxidized as follows:

$$Fe_3O_4 + 0.25O_2 + 4.5H_2O \rightarrow 3Fe(OH)_3 \quad (3)$$

affecting the physical and chemical properties of the nanosized magnetic particles.

Magnetite particles obtained under different synthetic conditions may display large heterogeneities regarding their magnetic properties. These differences are attributed to changes in structural disorder, creation of antiphase boundaries, or the existence of a magnetically dead layer at the particle surface [7].

Fig 2 shows the XRD patterns at room temperature of the Fe_3O_4 powder. The simulated XRD pattern of Fe_3O_4 generated using the Powdercell software is also shown. The structural model of bulk Fe_3O_4 was used for the simulation [8]. There is a good agreement between the measured and the simulated patterns, indicating that the sample consists of a single phase, Fe_3O_4.

The nanoparticles crystallize in cubic type structure (space group number 227) [8] as it is demonstrated by the position and the relative intensities of their diffraction peaks, matching well with the standard XRD data for bulk magnetite. There are no peaks of any other phases in the XRD patterns, indicating the high purity of the product. The lattice parameter is *a*=8.36 Å, smaller than the bulk one (*a*=8.397 Å). The sample show very broad peaks which are indicative for small crystallite size of nanoparticles. The average crystallite size was determined to be 24±1 nm.

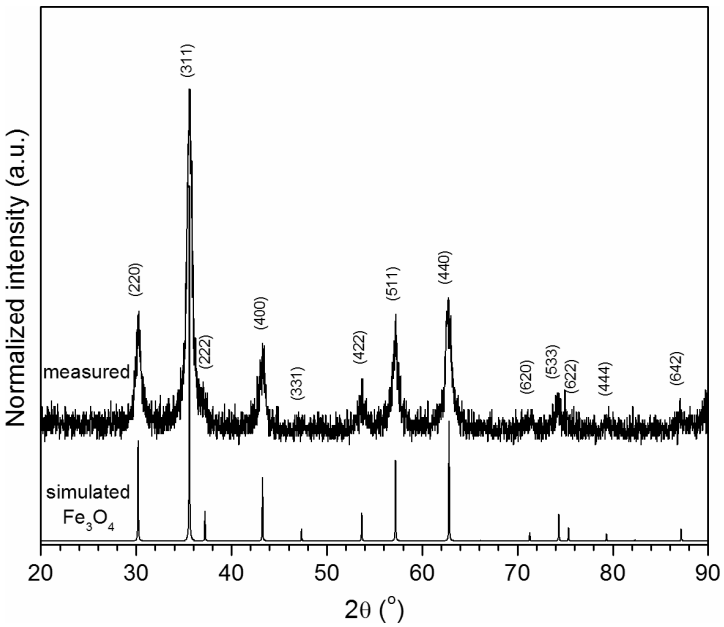

Fig. 2. XRD patterns of the of the Fe_3O_4 powder.

The magnetic measurements indicate that the Fe_3O_4 nanoparticles are ferrimagnetic at 4 K and at 300 K, too (see Fig.3). The saturation magnetization, M_S, values are 77 emu/g at 4 K, respectively 70 emu/g at 300 K. These values are lower than the value of bulk magnetite (~92 emu/g at room temperature [9, 10]) and they are comparable with previous reported M_S data [11-13]. The decrease of the saturation magnetization can be attributed to the disorder canting spins at the surface, due to the coordination number imperfections or to the formation of cation vacancies into the crystalline structure during the synthesis [14, 15]. The nanoparticle surface can be composed of some disordered or canted spins and these spins do not allow the core spins to be aligned along the external field direction. This results in a decrease of the saturation magnetization of these small sized nanoparticles.

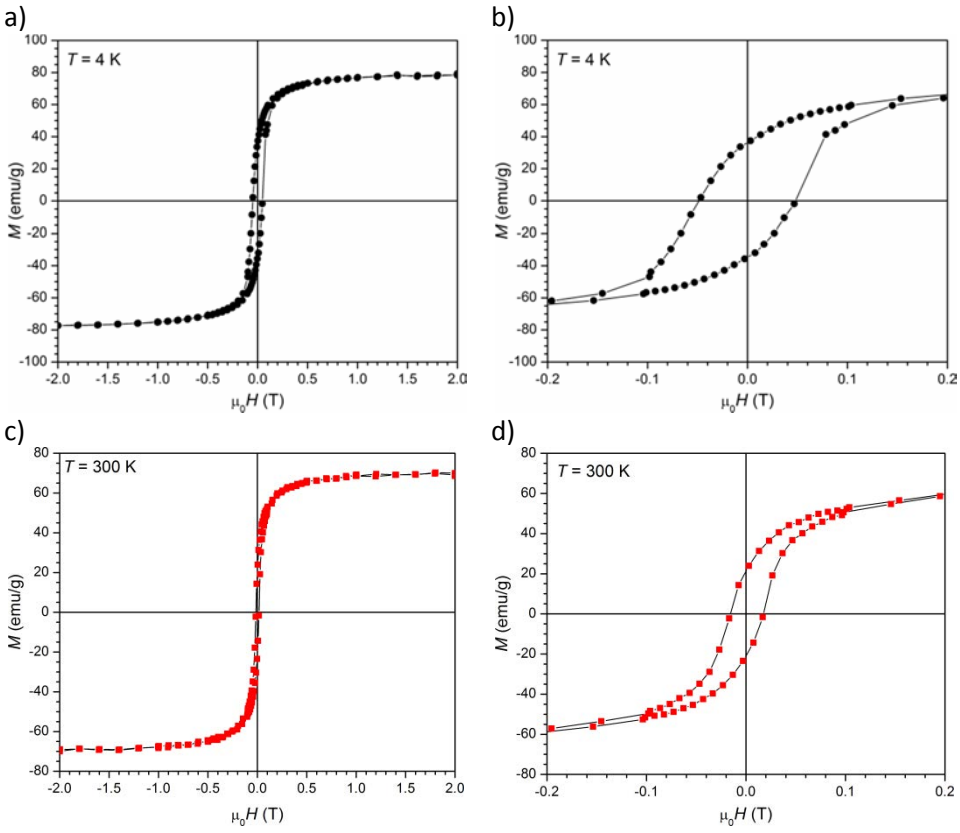

Fig. 3. Magnetic hysteresis loops recorded at 4 K and 300 K.

The coercive field is around 0.046 T at 4 K and decreases to 0.015 T at *T*=300 K which shows that the particles are not in a pure superparamagnetic state. The coercive fields values increase while the temperature decreased suggesting that the nanoparticle undergo a superparamagnetic to ferrimagnetic transition.

To get more insights into the magnetic behaviour, the thermal dependence of the magnetization in field cooling (FC) and zero field cooling (ZFC) has been recorded in a 0.05 T field between 4 K and 300 K. The ZFC curves show a broad maximum centred at around 133 K (see Fig.4) and below this temperature the magnetization decreases with decreasing temperature while the FC magnetization increase continuously down to 4 K. This behaviour indicates a gradual transition which corresponds to the average onset of the ferrimagnetic to superparamagnetic transition, even if the superparamagnetic state is not pure.

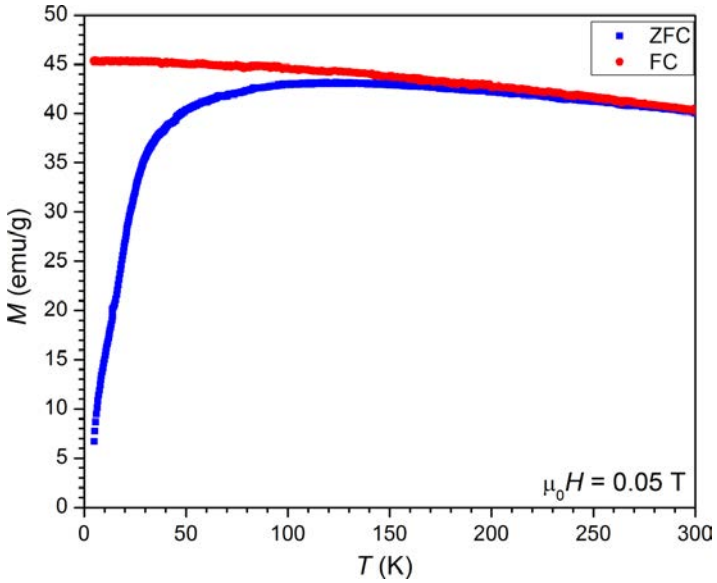

Fig. 4. Temperature dependence of zero-field cooled and field cooled magnetization in 0.05 T.

The M(T) values of FC curves can provide information about the inter-particle interaction strength [16]. It was reported that larger grain-sizes are favourable for stronger long-range ferromagnetic (FM) coupling, while grains with smaller sizes can create heavier strain at the grain boundaries and give rise to more non-FM or weak antiferromagnetic regions which can disturb the long-range FM order [17]. In our system, the true long-range FM coupling is absent due to the small grain size of the samples.

The magnetic properties suggest the possibility of using these nanoparticles on large scale applications.

CONCLUSIONS

Magnetite nanoparticles with crystallite average size of 24 nm were obtained by a simple synthesis route, at room temperature. The magnetic measurements indicate that the Fe_3O_4 nanoparticles are ferrimagnetic at 4 K and at 300 K, too. Their saturation magnetization, M_S, values being 77 emu/g at 4 K, respectively 70 emu/g at 300 K, lower values than the value of bulk magnetite. The coercive field values increase while the temperature decreases, suggesting that the nanoparticles undergo a superparamagnetic to ferrimagnetic transition. The coercive field was found to be around 0.046 T at 4 K and decreases to 0.015 T at T=300 K which indicates that the particles are not in a pure superparamagnetic state. The ZFC curve recorded between 4 K and 300 K shows a broad maximum centred at around 133 K and below this temperature the magnetization decreases with decreasing temperature, while the FC magnetization increases continuously, down to 4 K. This behaviour indicates a gradual transition which corresponds to the average onset of the ferrimagnetic to superparamagnetic transition, even if the superparamagnetic state is not pure.

ACKNOWLEDGMENTS

NL and AS acknowledge support from the Competitiveness Operational Programme 2014-2020 POC-A1-A1.1.4-E-2015, financed under the European Regional Development Fund, project number P37_245.

REFERENCES

1. V. Valdiglesias, N. Fernández-Bertólez, G. Kiliç, C. Costa, S. Costa, S. Fraga, M.J. Bessa, E. Pásaro, J.P. Teixeira, B. Laffon, *J. Trace Elem. Med. Biol*., 38, 53 (2016).
2. B. Issa, I.M. Obaidat, B.A. Albiss, Y. Haik, *Int. J. Mol. Sci*., 14, 21266 (2013).
3. I. Martínez-Mera, M.E. Espinosa-Pesqueira, R. Pérez-Hernández, J. Arenas-Alatorre, *Mater. Lett*., 61, 4447 (2007).
4. M. Yazdi, Z.N. Najafi, M. Khorramizadeh, M. Amini, A. Shahverdi, DARU, *J. Pharm. Sci.,* 20 (2012).

5. G.K. Williamson, W.H. Hall, *Acta Metall*, 1, 22 (1953).
6. I.J. Bruvera, P. Mendoza Zélis, M. Pilar Calatayud, G.F. Goya, F.H. Sánchez, *J. Appl. Phys.,* 118, 184304 (2015).
7. A.K. Gupta, M. Gupta, *Biomaterials*, 26, 3995 (2005).
8. N. Tzafaras, W. Adlhart, H. Jagodzinski, *Acta Cryst. A*, 37A, C-104 (1981).
9. A.G. Roca, J.F. Marco, M. Del Puerto Morales, C.J. Serna, *J. Phys. Chem. C*., 111, 18577 (2007).
10. B. Wang, Q. Wei, S. Qu, *International J. Electrochem. Soc.,* 8, 3786 (2013).
11. C. Salazar-Camacho, M. Villalobos, M.D.L.L. Rivas-Sánchez, J. Arenas-Alatorre, J. Alcaraz Cienfuegos, M.E. Gutiérrez-Ruiz, *Chem. Geol*., 347, 233 (2013).
12. W.S. Peternele, V. Monge Fuentes, M.L. Fascineli, J. Rodrigues Da Silva, R.C. Silva, C.M. Lucci, R. Bentes De Azevedo, *J. Nanomater*., 2014 Article ID 682985, (2014).
13. S. Rajput, C.U. Pittman, D. Mohan*, J. Colloid. Interface Sci*., 468, 334 (2016).
14. Y. Zhang, Z. Yang, D. Yin, Y. Liu, C. Fei, R. Xiong, J. Shi, G. Yan, *J. Magn. Magn. Mater.,* 322, 3470 (2010).
15. V. Kumar, A. Rana, M.S. Yadav, R.P. Pant, *J. Magn. Magn. Mater.,* 320, 1729 (2008).
16. I. Andreu, E. Natividad, L. Solozábal, O. Roubeau, *ACS Nano*, 9, 1408 (2015).
17. E. Taşarkuyu, A. Coşkun, A.E. Irmak, S. Aktürk, G. Ünlü, Y. Samanciolu, A. Yücel, C. Sarikürkçü, S. Aksoy, M. Acet, *J. Alloys Compd*., 509, 3717 (2011).